

*(Supporting Information)*

**Enhanced excitonic features in anisotropic ReS<sub>2</sub>/WSe<sub>2</sub> heterostructure**

Arslan Usman<sup>a</sup>, M. Adel Aly<sup>a,b</sup>, Hilary Masenda<sup>a,c</sup>, Joshua J.P. Thompson<sup>a</sup>, Surani M. Gunasekera<sup>d</sup>,  
Marcin Mucha-Kruczyński<sup>d,e</sup>, Samuel Brem<sup>a</sup>, Ermin Malic<sup>a</sup>, Martin Koch<sup>a</sup>

<sup>a</sup>*Department of Physics and Materials Sciences Centre, Philipps-Universität Marburg, 35032 Marburg, Germany*

<sup>b</sup>*Department of Physics, Faculty of Science, Ain Shams University, Cairo 11566, Egypt*

<sup>c</sup>*School of Physics, University of the Witwatersrand, 2050 Johannesburg, South Africa*

<sup>d</sup>*Department of Physics, University of Bath, Claverton Down, Bath BA2 7AY, UK*

<sup>e</sup>*Centre for Nanoscience and Nanotechnology, University of Bath, Claverton Down, Bath BA2 7AY, UK*

*\* Corresponding Author:*

*Arslan Usman (A. Usman) : arslan.usman@physik.uni-marburg.de*

Figures S1-S4.

Table 1: Parameters to calculate trion binding energy.

Note 1: Theoretical model and DFT input for calculation of exciton binding energy and wavefunction.

Note 2: Raman spectroscopy.

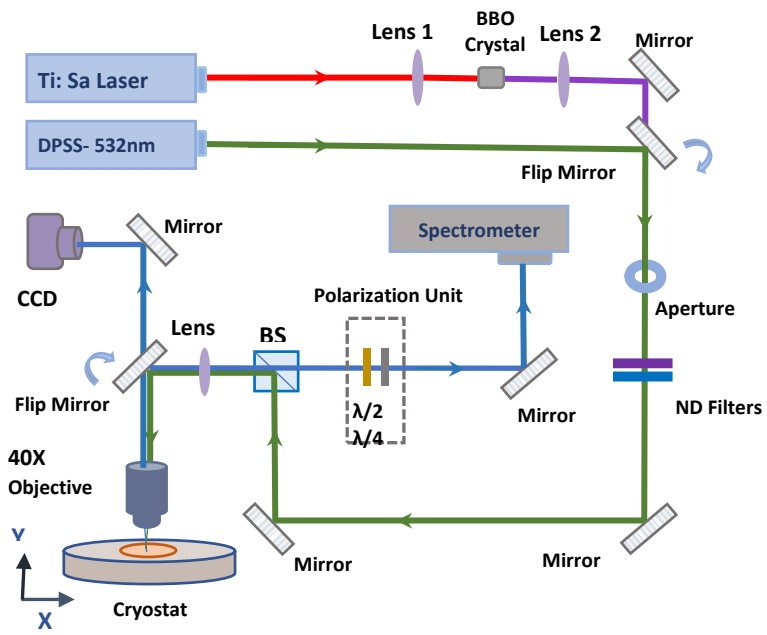


Figure S1: Schematic of PL and Polarization resolved measurement setup

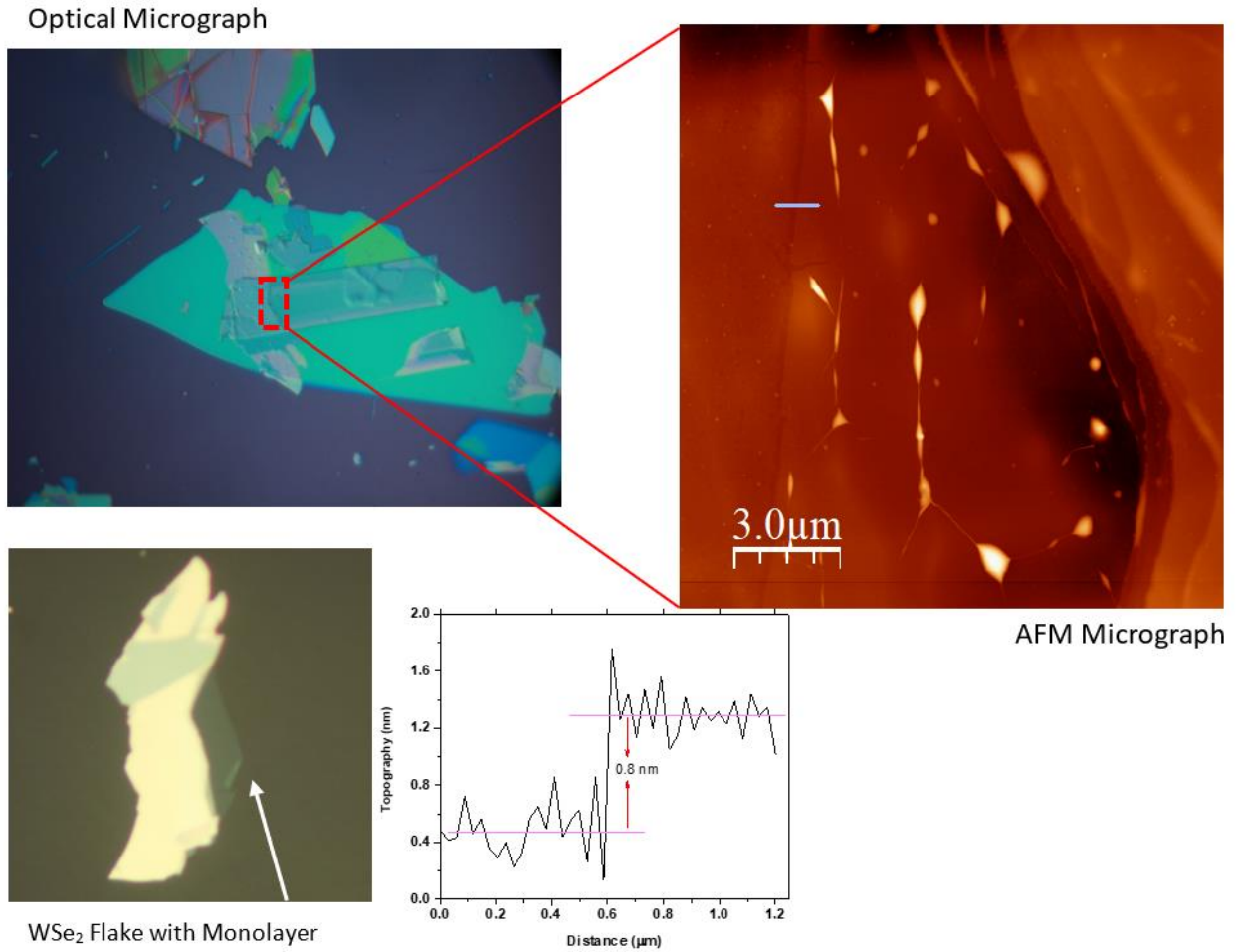


Figure S2: Optical and AFM micrograph of heterostructure along with line profile.

**Table T1: Parameters used to calculate trion binding energy**

$C_0$	-0.42 [1]
$C_1$	158 [1]
$C_2$	-1330 [1]
$C_3$	3113 [1]
$C_4$	-2640 [1]
$\mu$	0.59
$\epsilon$	6.8, 7.2 [2]

## N1- Theoretical model and DFT input for calculation of exciton binding energy and wavefunction

In this section we outline the theoretical method and DFT data to calculate the excitonic binding energy and wavefunctions.

We use DFT data to extract the effective mass, dielectric constant and crystal structure. DFT calculations were performed using the QUANTUM ESPRESSO [3] software, with scalar relativistic LDA pseudopotentials from the PSLibrary [4]. These pseudopotentials used the Perdew-Zunger parametrisation of the exchange-correlation energy [5] and were used with the projector augmented wave (PAW) method [6, 7]. The valence of Re was taken as 15, and no van der Waals' corrections were included. Initial atomic coordinates were taken from the Chemical Database Service [8] for monolayer ReS<sub>2</sub>. The kinetic energy cutoff was 60 Ry (816 eV) and Monkhorst-Pack [9] k-point meshes of 20x20x1 were used.

The lattice constant of monolayer ReS<sub>2</sub> is approximately 0.63 nm which comes from previous experimental works and ab initio calculations [10]. We use the calculated DFT electronic dispersion to find the effective mass of the anisotropic band structure. We extract the effective mass in the directions parallel to (x) and perpendicular to (y) the Re-chains in the monolayer.

For the conduction band we obtain

$$\begin{aligned} m_c^x &= 0.59m_o \\ m_c^y &= 1.66m_o \end{aligned}$$

For the valence band we obtain

$$\begin{aligned} m_v^x &= -2.42m_o \\ m_v^y &= -14.9m_o \end{aligned}$$

These values reflect the 1D-nature of the electronic motion along the Re-chains (b-axis) in the monolayer.

We were also provided with DFT data for the dielectric constant in ReS<sub>2</sub> which we expect to be anisotropic in the plane. Eliminating the vacuum contribution, we obtain the tensor

$$\epsilon = \begin{pmatrix} \epsilon_{xx} & 0 & 0 \\ 0 & \epsilon_{yy} & 0 \\ 0 & 0 & \epsilon_{zz} \end{pmatrix} = \begin{pmatrix} 14.06 & 0 & 0 \\ 0 & 13.29 & 0 \\ 0 & 0 & 4.61 \end{pmatrix}$$

where x lies along the Re chains in the monolayer, and z is out of plane. We use the Wannier equation to obtain the binding energies, modified to consider the band anisotropy and anisotropic dielectric screening in the TMD.

We rely on the assumption that around the band gap, the valence band maximum and conduction band minimum are approximately parabolic. From this we can employ the Wannier equation to calculate the excitonic binding energy.

$$\frac{\hbar^2(k_x^2 + k_y^2)}{2m_r^{xy}} \varphi_{k_x, k_y}^n + \sum_{q_x, q_y} V_{Kel}(k_x + q_x, k_y + q_y) \varphi_{q_x, q_y}^n = E_b^n \varphi_{k_x, k_y}^n$$

Here,  $E_b^n$  denotes the exciton binding energy with energy level  $n$ ,  $V_{Kel}$  is the screened Keldysh Coulomb interaction,  $\varphi_{k_x, k_y}^n$  the excitonic wavefunction, and  $m_r^{xy}$  the reduced mass which varies due to the anisotropy.

The calculation presented here is for freestanding ReS<sub>2</sub>, the presence of substrates (especially hBN encapsulation) should reduce the magnitude of the binding energy.

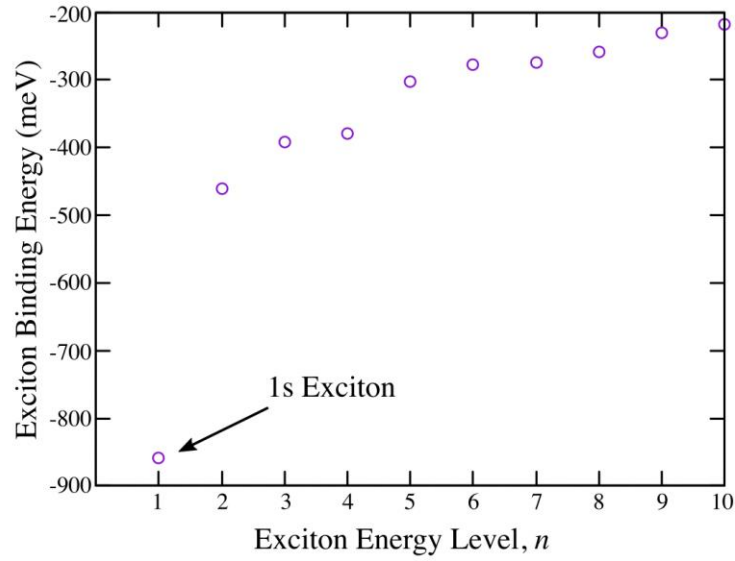


Figure S3: Binding energies,  $E_b^n$  for ReS<sub>2</sub>. The 1s-exciton has a binding energy of 859 meV.

## N2- Raman Spectroscopy

In  $\text{ReS}_2$  the spectral position of the Raman peak depends on the number of monolayers [11]. To determine the number of monolayers, present in our sample we performed a Raman spectroscopic analysis in back scattered geometry. It is carried out under ambient conditions using an Argon Ion laser (514 nm) which is focused onto the heterostructure with a 100x objective. The spectral resolution of the Raman setup is  $0.04 \text{ cm}^{-1}$ . Figure S4, shows characteristic vibrational spectra obtained for the monolayer as well as for the corresponding heterostructure. The spectra reveal the characteristic  $A_g^1$  mode of  $\text{WSe}_2$  along with the 2<sup>nd</sup> order longitudinal phonon mode.

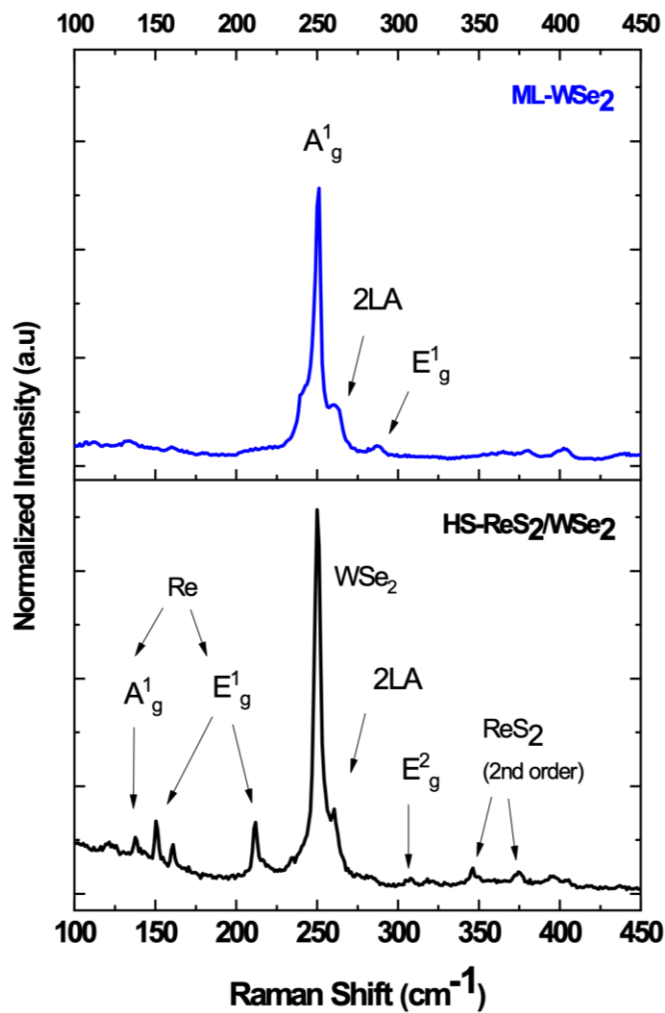


Figure S4: Raman spectra of the  $\text{WSe}_2$  monolayer and the corresponding heterostructure with FL-  $\text{ReS}_2$

These phonon modes are also visible in the heterostructure alongside with the  $\text{ReS}_2$  berating mode at  $260 \text{ cm}^{-1}$ . The distinct  $A_g^1$  mode of  $\text{ReS}_2$  corresponds to out-of-plane vibrations of Re atoms. The phonon distribution in few layer  $\text{ReS}_2$  seems to be nearly identical to that of bulk [12, 13]. This indicates

electronic and vibrational isolation of this material with respect to the number of layers. The in-plane vibrational mode of Re and S atoms can be seen at  $160\text{ cm}^{-1}$ ,  $212\text{ cm}^{-1}$  and  $308\text{ cm}^{-1}$ , respectively. It is also noticeable that the breathing mode is stronger than the shear mode in  $\text{ReS}_2$ , whereas the shear mode is dominating in conventional 2D materials [14, 15]. We could also quantify the number of  $\text{ReS}_2$  layers by analyzing the peak positions [16]. The peak at  $136\text{ cm}^{-1}$  indicates that there are 4-layers of  $\text{ReS}_2$  in our heterostructure. When the Raman frequency increases the vibrational atomic weights of Re and S atoms changes due to intrinsic difference of their atomic weights, this leads to variable Re-Re dimers and thus changes the bond charge polarization and generates different intensities [17].

#### References:

1. Thilagam A, *Physical Review B*, 1997, **56**, 4665.
2. Ankur Sharma, Han Yan, Linglong Zhang, Xueqian Sun, Boqing Liu, Yuerui Lu, *Accounts of Chemical Research*, 2018, **51**(5), 1164–1173.
3. P. Giannozzi, S. Baroni, N. Bonini, M. Calandra, R. Car, C. Cavazzoni, D. Ceresoli, G. L. Chiarotti, M. Cococcioni, I. Dabo, et al., *J. Phys.: Condens. Matter.*, 2009, **21**, 395502.
4. A. Dal Corso, *Comput. Mater. Sci.*, 2014, **95**, 337.
5. J. P. Perdew; A. Zunger, *Physical Review B*, 1981, **23**, 5048.
6. P. E. Blöchl., *Physical Review B*. 1994, **50**, 17953.
7. G. Kresse; D. Joubert, *Physical Review B*, 1999, **59**, 1758.
8. D. A. Fletcher; R. F. McMeeking; D. Parkin, *Journal of Chemical Information and Computer Sciences*. 1996, **36**, 746.
9. H. J. Monkhorst, J. D. Pack, *Physical Review B*, 1976, **13**, 5188.
10. S. M. Gunasekera. D. Wolverson; L. S. Hart, M. Mucha-Kruczyński, *J. Electron. Mater.* 2018, **47**, 4314–430.
11. Daniel A. Chenet, O. Burak Aslan, Pinshane Y. Huang, Chris Fan, Arend M. van der Zande, Tony F. Heinz, James C. Hone, *Nano Letters*, 2015, **15**, 5667–5672.
12. Yanqing Feng, Wei Zhou, Yaojia Wang, Jian Zhou, Erfu Liu, Yajun Fu, Zhenhua Ni, Xinglong Wu, Hongtao Yuan, Feng Miao, Baigeng Wang, Xiangang Wan, Dingyu Xing, *Physical Review B*, 2015, **92**, 054110.
13. Naktal Al-Dulaimi, David J. Lewis, Xiang Li Zhong, M. Azad Malik, Paul O'Brien, *Journal of Material Chemistry C*, 2016, **4**, 2312.
14. Takeshi Fujita, Yoshikazu Ito, Yongwen Tan, Hisato Yamaguchi, Daisuke Hojo, Akihiko Hirata, Damien Voiry, Manish Chhowalla, Mingwei Chen, *Nanoscale*, 2014, **6**, 12458-12462.
15. Etienne Lorchat, Guillaume Froehlicher, Stéphane Berciaud, *ACS Nano*, 2016, **10**, 2752–2760.
16. A. McCreary, J. R. Simpson, Y. Wang, D. Rhodes, K. Fujisawa, L. Balicas, M. Dubey, V. H. Crespi, M. Terrones, A. R. Hight Walker, *Nano Letters*, 2017, **17**, 5897.
17. Xiancui Su, Baitao Zhang, Yiran Wang, Guanbai He, Guoru Li, Na Lin, Kejian Yang, Jingliang He, Shande Liu, *Photonics Research*, 2018, **6**, 498-505.